Proceedings of the ASME 2013 11th Fuel Cell Science, Engineering and Technology Conference
FuelCell2013
July 14-19, 2013, Minneapolis, MN, USA

FuelCell2013-18070

EFFECT OF PTFE ON THERMAL CONDUCTIVITY OF GAS DIFFUSION LAYERS OF PEM FUEL CELLS

Hamidreza Sadeghifar
PhD candidate
Mechatronic Systems Engineering,
School of Engineering Science,
Simon Fraser University,
Surrey V3T 0A3, BC, Canada
hamidreza_sadeghifar@sfu.ca

Ned Djilali
Professor
Department of Mechanical Engineering,
University of Victoria,
Victoria V8W 3P6, BC, Canada
ndjilali@uvic.ca

Majid Bahrami *
Associate Professor
Mechatronic Systems Engineering,
School of Engineering Science,
Simon Fraser University,
Surrey V3T 0A3, BC, Canada
mbahrami@sfu.ca

ABSTRACT

Through-plane thermal conductivity of 14 SIGRACET gas diffusion layers (GDLs), including series 24 & 34, as well as 25 & 35, are measured under different compressive pressures, ranging from 2 to 14 bar, at the temperature of around 60 ℃. The effect of compression, PTFE loadings, and micro porous layer (MPL) on thermal conductivity of the GDLs and their contact resistance with an iron clamping surface is experimentally investigated. The contact resistance of MPL coated on GDL with the substrate of that GDL is measured for the first time in this paper. A new robust mechanistic model is presented for predicting the through-plane thermal conductivity of GDLs treated with PTFE and is successfully verified with the present experimental data. The model can predict the experimentally-observed reduction in thermal conductivity as a result of PTFE treatment and provides detailed insights on performance modeling of PEMFCs.

KEY WORDS:
Gas diffusion layer, microstructure modeling of fibrous porous media, through-plane thermal conductivity, thermal contact resistance, PTFE, MPL

INTRODUCTION

The efficiency and performance of proton exchange membrane fuel cells (PEMFCs) depends heavily on the heat and associated water imbalances because of their low operating temperature, which is typically less than 100 ℃ [1-5]. One of the parameters that directly affects both heat and water management of a PEMFC, as well as durability and longevity of its components, is the temperature distribution inside the membrane electrode assembly (MEA) [6-11]. This temperature distribution is highly dependent on the thermal conductivity of fuel cell components, especially gas diffusion layer (GDL) [12-14]. Hence, accurate prediction of the GDL thermal conductivity and investigating its dependency on salient parameters such as compression, micro-structured characteristics, additive materials of Polytetrafluoroethylene (PTFE) and micro porous layer (MPL) are vital for understanding and improving the performance and longevity of PEMFCs.

GDLs are usually treated with different loads of hydrophobic PTFE for the purpose of water management. However, the added PTFE can change the thermal resistance of GDLs and, hence, affects the fuel cell heat management as well. Few studies have been to date performed to measure and model the thermal conductivity of GDLs treated with PTFE. Khandelwal and Mench [15] and Burheim et al. [16-17] reported that the PTFE treatment leads to a reduction in the GDL thermal conductivity whereas Zamel et al. [12] did not observe any changes in GDL thermal conductivity with a PTFE addition of as high as 60 wt%. As for the modeling, the models developed by Yablecki and Bazylak [18] and Fishman and Bazylak [19] both predict a noticeable increase in thermal conductivity of GDLs with increasing PTFE content. As it will be shown in the present study, such predictions are not consistent with experimental data. As such, in this paper, we propose a mechanistic model that enables accurate prediction of the thermal conductivity of PTFE-treated GDLs.

The present model results are compared and successfully validated with thermal conductivity of several SIGRACET GDLs treated with a range of PTFE content. In addition, the

effect of MPL on thermal conductivity and thermal contact resistance of GDLs is investigated experimentally. Moreover, the contact resistance of MPL with GDL substrate, which has been overlooked in the literature so far, is measured for the first time in this paper.

NOMENCLATURE

A	Cross-sectional area of sample or fluxmeters, m^2
AA	SIGRACET GDL with 0 wt% PTFE
BA	SIGRACET GDL with 5 wt% PTFE
DA	SIGRACET GDL with 20 wt% PTFE
BC	SIGRACET GDL with 5 wt% PTFE, MPL on one side
d	Fiber diameter, m
GDL	Gas Diffusion Layer
k	Thermal conductivity, $Wm^{-1} K^{-1}$
k_{eff}	Effective thermal conductivity, $Wm^{-1} K^{-1}$
k_{FM}	Thermal conductivity of fluxmeter , $Wm^{-1} K^{-1}$
l	Distance between fibers in the x-direction, m
MPL	Micro Porous Layer
P	Compression pressure, bar
PEMFC	Polymer electrolyte membrane fuel cell
PTFE	Polytetrafluoroethylene
PTFE′	PTFE trapped between two fibers at their conjunction at the upper block of the unit cell
PTFE″	PTFE trapped between two fibers at their conjunction at the lower block of the unit cell
PTFE‴	PTFE extended along fibers
$PTFE_{layer}$	A thin layer of PTFE on the fibers of the first and last layers of GDL
Q	Heat transfer through the fluxmeters, W
R	Thermal resistance, KW^{-1}
SGL	SIGRACET
T	Temperature, K
t	thickness, m
TCR	Thermal contact resistance, KW^{-1}
Wt%	Weight percent
x	Position of thermocouples inside fluxmeters
R_{sp}	Spreading resistance, KW^{-1}
R^*	thermal resistance correction factor, KW^{-1}
T	Temperature, K
w	distance between two fibers in the y direction, m

Superscript

MPL	Micro porous layer
eff	Effective value
tot	total
sub	GDL substrate
GDL	Gas Diffusion Layer
g	Gas (see [20-21])
gc	Gas filled gap (see [20-21])
1	Related to thickness 1 or block 1 of unit cell (see [20-21])
2	Related to thickness 2 or block 2 of unit cell (see [20-21])

2. MODEL DEVELOPMENT

A statistically-based mechanistic robust model has already been developed by the same authors in [20] for predicting the through-plane thermal conductivity of *untreated* GDLs. The untreated GDL model took into account the effects of salient geometrical parameters and operating conditions on thermal conductivity, also considered the spreading/constriction resistances between touching fibers [20-21]. This model will be modified to account for the PTFE treatment of GDLs. Based on images from inside GDLs treated with PTFE, such as the ones shown in Fig. 1, one can notice a considerable portion of PTFE are accumulated at the intersection of fibers (Fig. 1b). For convenience, we call this portion PTFE′ and PTFE″, the upper and lower halves in the through-plane directions, respectively. In addition, some PTFE (PTFE‴) cover each fiber randomly (Fig. 1a and c) and a thin layer of PTFE on the first and last layers of fibers in the GDL ($PTFE_{layer}$) can be seen (Fig. 1a). Accordingly, we assume a distribution for the geometrical modeling of PTFE-treated GDLs as illustrated in Fig. 2. As seen in Fig. 2, the PTFE only penetrates into a few layers of the GDL at each side, i.e., the middle layers do not contain any PTFE. This assumption is consistent with the PTFE treatment procedure used in industry, which is dipping the GDL in a pool of PTFE. It should also be noted that the fiber and angle distribution and other characteristics of GDL fibers will not be changed as a result of PTFE treatment. As mentioned, we successfully considered these characteristics of GDL in our previous study [20] for untreated GDLs.

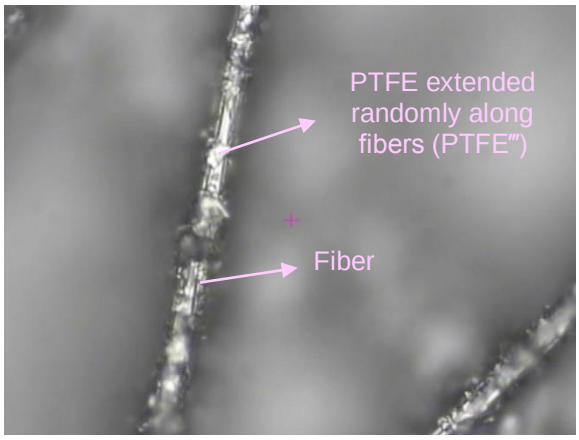

(a)

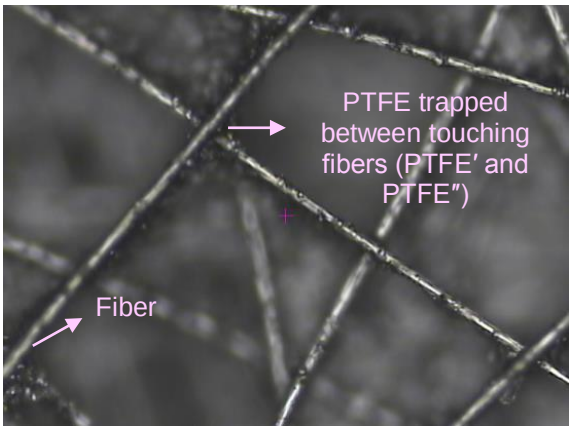

(b)

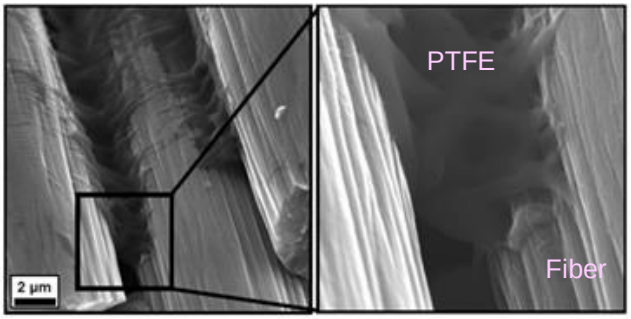

(c)

Fig. 1: PTFE distribution inside different GDLs: (a) and (b) SGL 24BA (present study) and (c) ELAT [22]

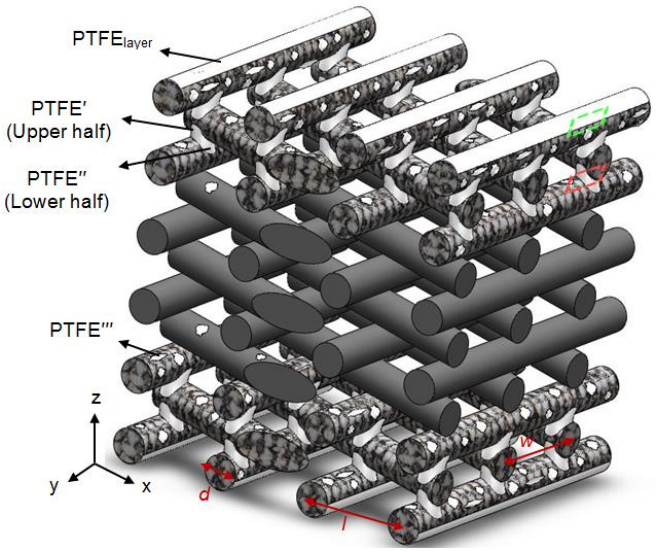

Fig. 2: Present geometrical model of GDLs treated with PTFE, see Eq. (1)

In general, the present model is based on a unit cell approach that considers a GDL as a periodic fibrous micro structure [20-21]. Similarly to the unit cell defined in [20-21] for untreated GDLs, a unit cell consisting two blocks is taken here for those fiber layers containing PTFE and another unit cell for the thin PTFE layers on both surfaces of GDLs, as shown in Figs. 2 and 3.

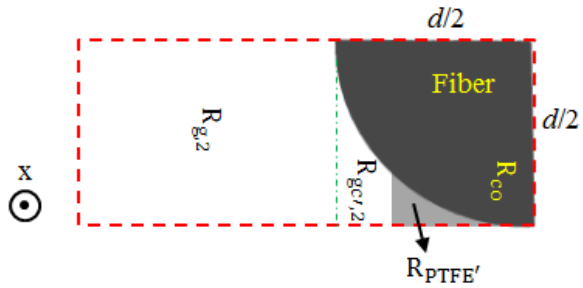

(a) Top block of the unit cell for the PTFE-treated fiber layers inside GDL (also see Fig. 2)

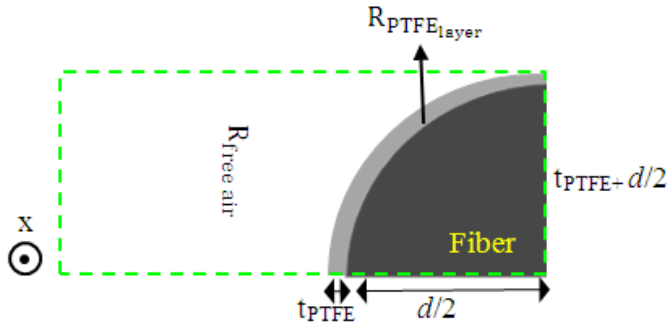

(b) The unit cell for the first and last fiber layers (also see Fig. 2)

Fig. 3: Unit cells and top block defined for a PTFE-treated GDL

For a GDL treated with PTFE, the thermal resistance network of the entire GDL, is depicted in Fig. 4a-c, will be:

$$R_{tot} = 2\left(\frac{1}{R_{free\ air}} + \frac{1}{R_{PTFE\ layer}}\right)^{-1} + \frac{n_{with\ PTFE}}{2}\left[\frac{1}{R_{g,1}+R_{PTFE'''}} + \frac{1}{R_{gc',1}} + \frac{1}{R_{1,PTFE''}} + \frac{1}{R_{co}}\right]^{-1} + \frac{n_{with\ PTFE}}{2}\left[\frac{1}{R_{g,2}} + \left(\frac{1}{R_{gc',2}} + \frac{1}{R_{2,PTFE'}}\right) + \frac{1}{R_{sp}}\right]^{-1} + \frac{n_{without\ PTFE}}{2}\left[\frac{1}{R_{g,1}} + \frac{1}{R_{gc,1}} + \frac{1}{R_{co}}\right]^{-1} + \frac{n_{without\ PTFE}}{2}\left[\frac{1}{R_{g,2}} + \frac{1}{R_{gc,2}} + \frac{1}{R_{sp}}\right]^{-1} \quad (1)$$

where all the resistances of R_{co}, R_{sp}, $R_{g,1}$, $R_{g,2}$, $R_{gc,1}$, $R_{gc,2}$, $R_{gc',1}$, and $R_{gc',2}$ have already been defined in [20-21], and $R_{PTFE\ layer}$ and $R_{free\ air}$ are as follows:

$$R_{PTFE\ layer} = \frac{t_{PTFE}}{k_{PTFE}\frac{\pi d(l+w)}{4}} \quad (2)$$

$$R_{free\ air} = \frac{\frac{d}{2} + t_{PTFE}}{k_{air}\frac{(l-d)(w-d)}{4}} \quad (3)$$

where k_{PTFE} and k_{air} are thermal conductivities of PTFE and air, respectively, and t_{PTFE} is the average thickness of PTFE coating on the fibers of the first and last layers of GDL, given later in Table 1. *l*, *w*, and *d* are the geometrical parameters shown in Fig. 2, which have already been given in [20] for the studied GDLs.

Note that all PTFE resistances inside the GDL, i.e., $R_{PTFE'}$, $R_{PTFE''}$, and $R_{PTFE'''}$, are in parallel to a much lower resistance, that is, conduction through fiber-fiber contacts , therefore, will not have a noticeable impact on the total resistance of the GDL, see Eq. (1). Accordingly, these PTFE resistances are secondary effects thus not needed for estimating the total resistance of the entire GDL. Note also that although the thermal conductivity of PTFE is one order of magnitude higher than that of air (k_{air}=0.026<k_{PTFE}=0.3 W m^{-1} K^{-1} [3]), it is still some orders of magnitude lower than the thermal conductivity of the fibers. As such, one can conclude that PTFE treatment on GDLs can be modelled as a "thin layer" on top/bottom layers of GDLs and will only effect the through plane thermal conductivity and the thermal contact resistance at the interface of GDL-bipolar plate. For this reason, the PTFE distributed inside the GDL does not have a noticeable impact on the through-plane thermal conductivity (also see [20]). Hence, from the viewpoint of through-plane heat transfer, the thermal resistance of a PTFE-treated GDL can be practically approximated in terms of untreated GDL, PTFE, and gas (air) resistances as:

$$R_{tot}^{PTFE-treated\ GDL} \simeq (n-1)R_{tot}^{Untreated\ GDL} + 2\left(\frac{1}{R_{free\ air}} + \frac{1}{R_{PTFE\ layer}}\right)^{-1} \quad (4)$$

where n is the number of fiber layers (=t_{GDL}/d).

The thermal conductivity of GDL can finally be calculated by:

$$k_{eff} = \frac{4t_{GDL}}{lwR_{tot}} \quad (5)$$

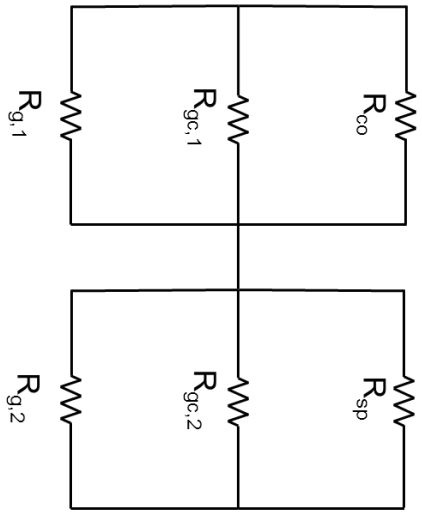

(a) Resistances of layers without PTFE (middle layers) (the negligible bulk resistance of fibers has been omitted)

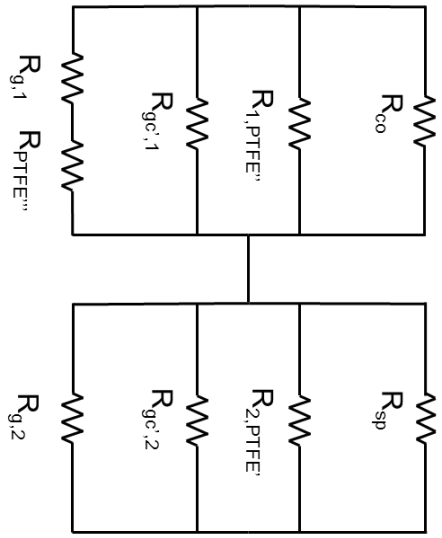

(b) Resistances of layers with PTFE (the negligible bulk resistance of fibers has been omitted)

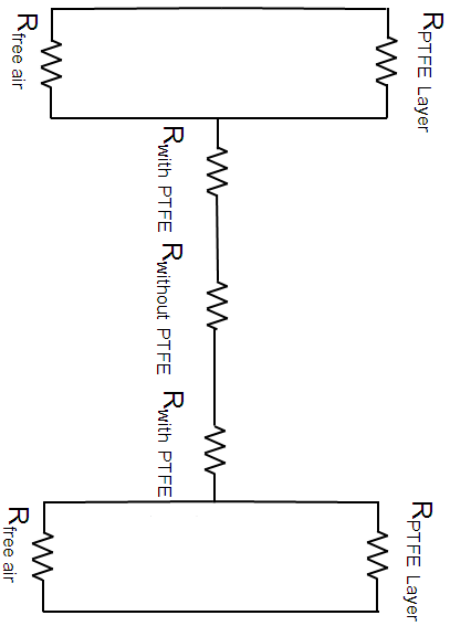

(c) The total thermal resistance network of the GLD treated with PTFE

Fig. 4: Thermal resistance network for a PTFE-treated GDL

3- Experimental study

3-1. GDL samples

Different treated and untreated SIGRACET gas diffusion layers, series SGL 24 and 34, as well as 25 and 35, are tested to obtain their thermal conductivity. The advantage of working with this type of GDLs is that the effect of PTFE and MPL on their thermal resistances can be separately investigated. Substrates of SGL BA and DA are fabricated by adding 5 and 20 wt.% PTFE to the *plain* (untreated) substrate AA, respectively, and the BC type is the BA substrate with MPL on one side, see Fig. 5 [24]. The numbers 24 and 34, as well as 25 and 35, included in the GDL names, refer to their thicknesses, as reported in Table 1. Hence, the only difference between the substrates of SGLs 24 and 34 and those of SGLs 25 and 35 is their thicknesses, which makes the two thickness method [14,20] an appropriate approach for measuring their thermal conductivity and contact resistance.

Fig. 5: SGL AA, BA, DA, and BC (the black layer represents MPL) with different PTFE loadings

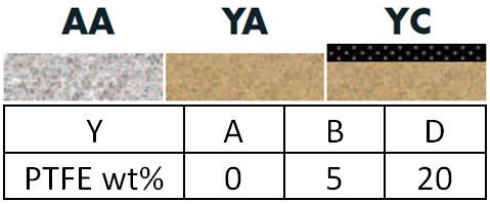

- GDLs with MPL on one side

GDLs coated with MPL on one side, such as SGL BC types, or on both sides [26-27], provide better electrical contacts between the GDL and catalyst or BPP and reduce ohmic losses, as the main component of MPL is the high electrical conductive material of carbon black. However, due to the very low thermal conductivity of carbon black and the hydrophobic agent of PTFE mixed with it, MPL may adversely influence the heat transfer in the fuel cell stack. As a result, knowing the thermal conductivity of MPL, as well as its thermal contact resistance with the GDL substrate, can be useful to the heat management of fuel cells. However, due to the complication associated with separation of this layer from the substrate, experimental measurements of its thermal conductivity can be troublesome [28]. Despite this problem, the thermal conductivity of MPL coated to the substrate is measured in the present study using the procedures explained in the following.

Table 1: Specifications of SIGRACET GDLs studied in the present work

SGL	24				25			34				35		
	AA	BA	DA	BC	AA	BA	BC	AA	BA	DA	BC	AA	BA	BC
Porosity (%)	88	84	72	76	92	88	80	88	84	72	76	92	88	80
Thickness (µm) ±5	190	190	190	235	190	190	235	280	280	280	315	300	300	325
PTFE Thickness on each surface (µm)	0	1.5	3	-	0	1	-	0	1.5	3	-	0	1	0

The total thermal resistance inside a GDL treated with MPL, as shown in Fig. 6, can be written as:

$$R_{GDL} = R_{sub} + R_{MPL} + TCR_{sub-MPL} \quad (6)$$

It is important to note that there is a contact resistance between the GDL substrate and MPL, $TCR_{sub-MPL}$, which has been overlooked in all the previous studies to determine the MPL thermal conductivity, see e.g. [29-31]. This resistance should be deconvoluted from the bulk resistance of the MPL, as performed in this study using the two thickness method. Having measured the thermal resistance of a GDL coated with MPL, the thermal bulk resistance of the MPL and its thermal contact resistance with the GDL substrate can be obtained using the two-thickness method.

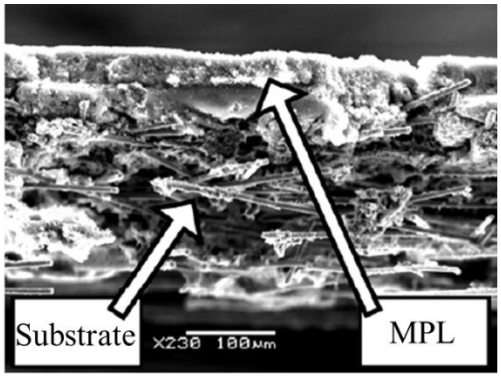

Fig. 6: A SEM image of the cross-section of a GDL containing MPL (substrate/MPL assembly) [25]

3-2. Apparatus and measurement principle

All thermal conductivities measurements are performed using a custom-built thermal contact resistance (TCR) machine, whose design is based on the principle of the guarded heat fluxmeter device recommended by the ASTM Standard D-5470–06 [32]. The details of the testbed and the principle of conducting the experiments can be found elsewhere [33-35].The principle utilized in thermal resistance measurements in this study is based on precise de-convoluting of the contact resistance of GDLs with clamping surface from their bulk resistances using the two-thickness method. Detailed explanations on the principle of the thermal contact resistance can be found elsewhere [36-41].

3-3. Testbed accuracy

Using two Pyrex 7740 calibration samples with different thicknesses, which have thermal resistances in the same order of magnitude of typical GDLs, the accuracy of the TCR machine was verified. The test results were very satisfactory, as the average measurement deviation was approximately 5% and the maximum measurement difference observed was 8%.

3-4. Uncertainty analysis

The uncertainty in the total resistance and thermal conductivity measurements of the test apparatus can be calculated in the same approach as performed in [14-15,26, 33-35]. The resistance and thermal conductivity are functions of the following parameters:

$$R \text{ or } k = f(Q, \Delta T, t, A, P, k_{FM}, x) \quad (7)$$

The maximum uncertainty for the thermal resistance and conductivity measurements can be calculated from

$$\frac{\delta R}{R} \text{ or } \frac{\delta k}{k} = \sqrt{(\frac{1}{2})(\frac{\delta Q}{Q})^2 + (\frac{\delta \Delta T}{\Delta T})^2 + (\frac{\delta t}{t})^2 + (\frac{\delta A}{A})^2 + (\frac{\delta P}{P})^2 + (\frac{\delta k_{FM}}{k_{FM}})^2 + (\frac{\delta x}{x})^2} \quad (8)$$

All the parameters and the uncertainty associated with them have been thoroughly defined in previous similar works [25,34] and are summarized in Table 2. Note that the main uncertainty in the experiments is related to heat flow rate passing through the fluxmeters, Q. The maximum uncertainty observed in this study was ±6.6 %.

Table 2: Uncertainty of involving parameters in the thermal resistance measurements in the present study

$\frac{\delta Q}{Q}$	$\frac{\delta \Delta T}{\Delta T}$	$\frac{\delta t}{t}$	$\frac{\delta A}{A}$	$\frac{\delta P}{P}$	$\frac{\delta k_{FM}}{k_{FM}}$	$\frac{\delta x}{x}$
0.0657	0.0031	0.0005	0.0015	0.05	0.0027	0.01

4- RESULTS AND DISCUSSION

Using the two thickness method, the thermal conductivity of the GDLs and their thermal contact resistance with the Armco-iron clamping surface (fluxmeters) has been obtained as a function of compression. In the following sections, the effect of PTFE loading (content), MPL, and compression on thermal resistances will be thoroughly discussed.

4-1. Effect of PTFE

- Model validation

The thermal conductivities of SGL 24 & 34 AA, BA, DA, and BC and those of series 25 & 35 AA, BA, and BC measured in this study are shown in Fig. 7. Comparing the model results with the experimental data of the PTFE-treated GDLs indicates that the present model predicts accurately the thermal conductivities of different GDLs. More importantly, the model captures the trend of the data, i.e., as the PTFE content increases the through-plane thermal conductivity of GDL decrease.

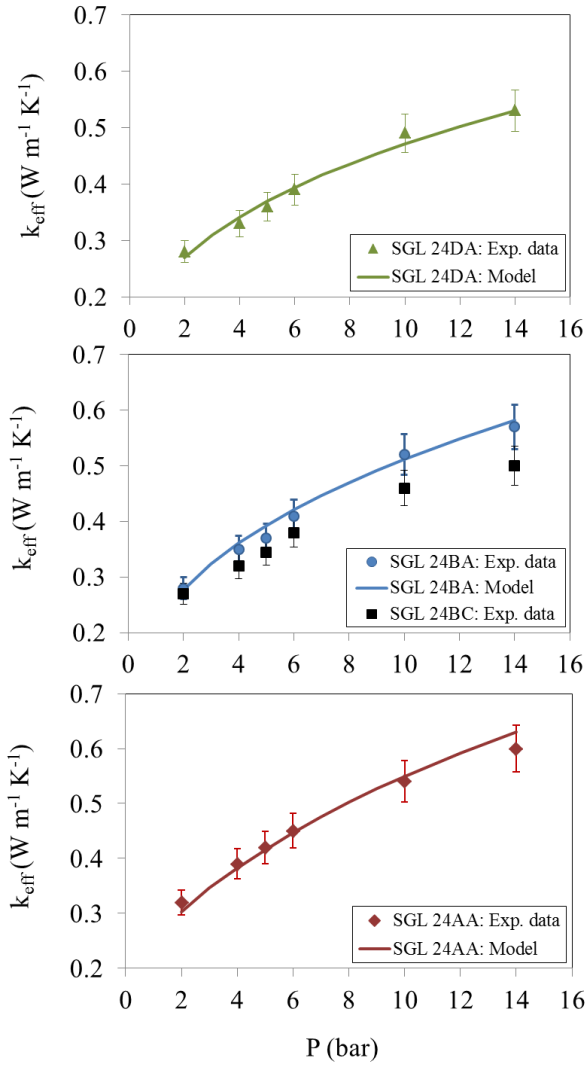

(a) SGLs 24AA (0% PTFE), 24BA (5% PTFE), 24BC (5% PTFE & MPL), and 24DA (20% PTFE)

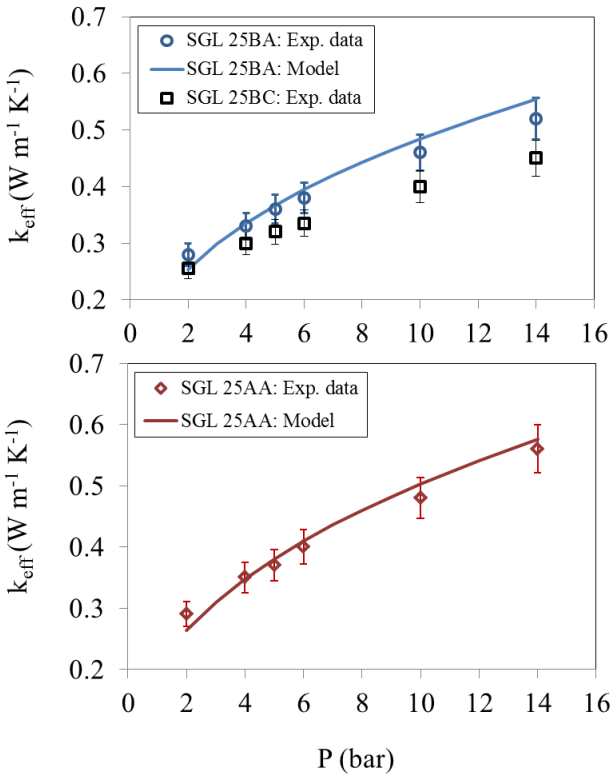

(b) SGLs 25AA (0% PTFE), 25BA (5% PTFE), and 25BC (5% PTFE & MPL)

Fig. 7: Comparison of the model results with experimental thermal conductivities of the studied GDLs with different PTFE loadings

From Fig. 7, the effect of different PTFE loading on the through-plane thermal conductivity can also be investigated experimentally. As can be seen, for each GDL, with increasing PTFE, the thermal conductivity decreases. This reduction can be attributed to the low thermal conductivity of PTFE, which increases the overall thermal resistance of the entire GDL. The trend observed here is in qualitative agreement with the results of Khandelwal and Mench [15] and Burheim *et al.* [16-17], but not with the very negligible reduction effect of 60 wt% PTFE on thermal conductivity reported in [12]. The reduction effect of PTFE on thermal conductivity is not consistent with the model predictions of Yablecki and Bazylak [18] and Fishman and Bazylak [19], where the thin layer of PTFE accumulated on the surface of the first and last fiber layers have been overlooked. In fact, the authors of [18-19] accounted for only the PTFE distributed inside the GDL in their modelling, which does not have a noticeable impact on through-plane thermal conductivity. It should be noted that although the PTFE added to the GDL displaces air, a lower thermal conductivity material, and decreases the GDL porosity, it does not enhance the overall thermal conductivity of the GDL, as discussed here and earlier in the Model Development Section.

It is interesting to note that the highest decrease observed in thermal conductivity on Fig. 7 is pertained to an increase in PTFE from 5 to 20 wt%. The effect of 5% PTFE loading on thermal conductivity is found to be negligible, as the curves of substrates AA (0% PTFE) and BA (5% PTFE) almost overlap or are very close to each other. The general trend of PTFE loading in thermal conductivity reduction is the same for the two series of the studied SGL GDLs, which can be accurately explained and interpreted with the analytical modeling as presented.

It is also worth mentioning that, unlike the through-plane thermal conductivity, the in-plane one does not decrease with

PTFE, rather slightly increases, as observed in [35]. The reason for this is that the very thin layer of PTFE covering the fiber layers on both surfaces of GDL will only influence the GDL thermal resistance in the through-plane direction and does not have an impact on that in the in-plane direction. However, since the low thermal conductivity material of air will be replaced by PTFE, it is expectable to see a slight increase in the in-plane thermal conductivity, as experimentally observed and analytically indicated in [35] (see Fig. 8). However, Zamel et al. [13] have reported a trend in contrast to the one observed in [35]. The reason for this may be due to the fact that the heat capacity and, finally, the thermal conductivity of the GDLs studied in [13] were estimated using a simple mixing rule instead of a direct measurement as an effective bulk value. In addition, the method employed for the thermal conductivity measurements in [13] was a transient method, which is believed not to be an appropriate measurement technique for application to thermal conductivity in porous materials [14,42].

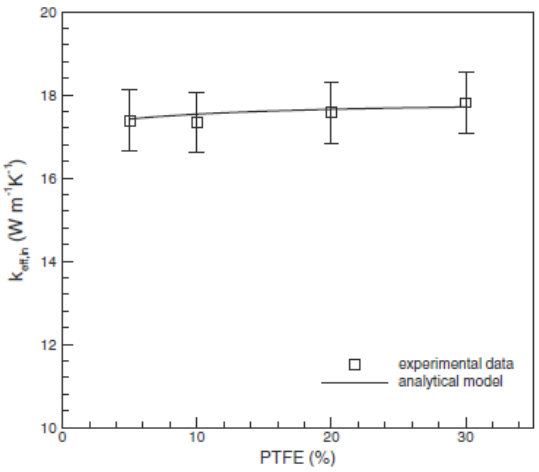

Fig. 8: In-plane thermal conductivity of Toray carbon paper TGP-H-120 over a range of PTFE content [35]

- Thermal contact resistance of PTFE-treated GDLs

The data of the thermal contact resistance between each of GDLs and the iron fluxmeters have been shown in Fig. 9. As seen, PTFE increases the thermal contact resistance. It can also be observed that at lower compressive pressures, interestingly enough, the thermal contact resistance is much sensitive to PTFE content. In other words, with increasing compression, the effect of PTFE on thermal contact resistance decreases. In general, these data can provide, at least, qualitative insights into the thermal contact resistance between a metallic bipolar plate [43] and GDLs, as function of PTFE loadings, compression, porosity, and characteristic fiber spaces.

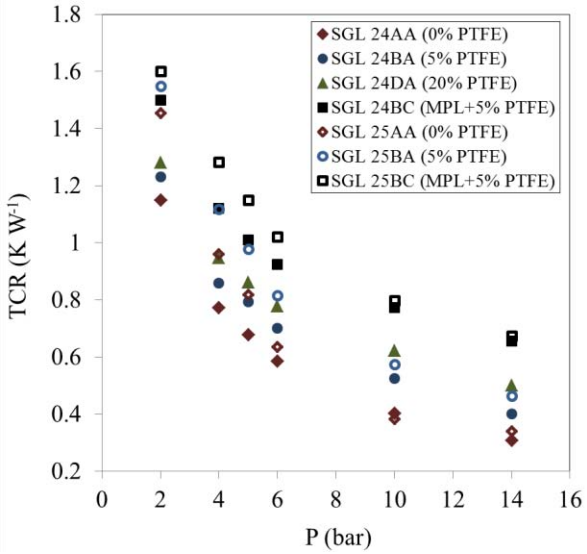

Fig. 9: Thermal contact resistance of different GDLs with the iron clamping surfaces as a function of compression: effect of PTFE loadings and MPL

4-2. Effect of MPL

The SGL GDLs of type BC are fabricated with coating a MPL on one side of SGL BA having 5 wt% PTFE. In order to accurately determine the effect of MPL on the thermal conductivity of GDLs and their contact resistances with other materials, the result of BC type of SGL GDLs should be compared with those of BA type. From Figs. 7 and 9, it can be observed that MPL reduced the thermal conductivity to some extent and increased the contact resistance dramatically. This finding is in qualitative agreement with [14] but not with the result of another study conducted in the same group on the same type of GDL (SolviCore) [25] reporting a negligible contact resistance of MPL with iron clamping surfaces. This uncorroborated finding of [25] was attributed to the high surface contact area of the MPL. It is worth mentioning that, unlike the present study, none of the previous studies performed for measuring the MPL thermal conductivity [14,17,25] takes the TCR between MPL and substrate into account. In addition, the tests of [14,25,33] have not been performed in a vacuum chamber and the thermal contact resistance between the stacked GDLs has also been simply omitted. The results of this study can shed light into the significant adverse impact of MPL on the heat transfer within MEA layers of PEMFCs.

- Thermal resistances inside GDLs containing MPL

Figure 10, illustrating the contribution of each resistance in Eq. (6) into the total resistance of the GDLs SGL 24BC and 25BC, reveals that the thermal contact resistance between substrate and MPL is comparable with the resistance of the MPL itself. It should be noted that the thickness of substrate in SGL BC is several times (~7 times) higher than that of MPL. Assuming the same thickness of MPL and substrate, it would be argued that the thermal contact resistance between substrate

and MPL, which is independent of the thickness of either component, can weigh even more than either of the substrate and MPL resistances.

Figure 10 also shows that with increasing the compression pressure up to 10 bar, the impact of MPL on contact resistance and also on the GDL thermal conductivity, and in general, the contribution of MPL to the increased total resistance, increases. Note that the contribution of MPL resistance to the GDL resistance is proportional to the ratio of the MPL thickness to the substrate one. For GDL substrates with thermal conductivities sufficiently higher than the MPL thermal conductivity, this ratio should be kept as low as possible in order to reduce the adverse influence of MPL on the bulk thermal conductivity of the GDL.

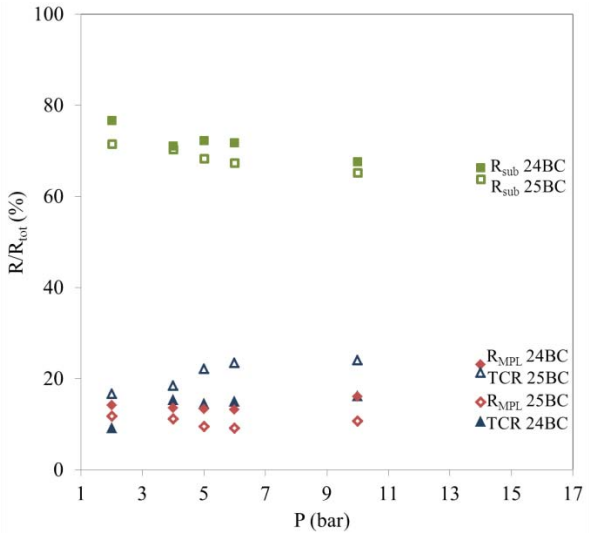

Fig. 10: Contribution of bulk and interfacial resistances inside a GDL containing MPL (Eq. (6))

4-3. Effect of compression

As can be observed from Figs. 7 and 9, the thermal conductivity of all the GDLs increases with compression whereas their thermal contact resistance with the clamping surface decreases. These reductions in the bulk and contact resistances can be attributed to a better contact between fibers of two adjacent layers and between the GDL and the iron clamping surface (fluxmeters) under higher compression, respectively.

- Thickness variation with compression

Carbon-based Gas diffusion layers, typically made of 30-50 layers of carbon fibers attached to each other, are of thicknesses ranging from 150 to 500 µm. Because of the porous nature of the GDL and elastic nature of the carbon fibers, the thickness of GDLs notably changes with compression. Fig. 11 shows the variations in thickness of the studied GDLs as a function of pressure, up to 15 bar. As observed from Fig. 11, the curve for each GDL can be divided into two non-linear, almost exponential, and linear parts. For pressures up to almost 7 bar, the variations in thickness of the studied GDLs are exponentially, depicting that the sharp reduction in thickness with increasing compression occurs at this range of compression. When the pressure increases from 7 to 15 bar, a relatively linear trend for the thickness variations with compression can be seen. The trends observed here for the SGL GDLs conform to the ones reported for other GDLs in the literature, such as [14,23,44]. However, these trends differ from those of Unsworth et al. obtained for SolviCore GDLs with and without MPL [25], where *linear* trends have been reported in the entire range of compression.

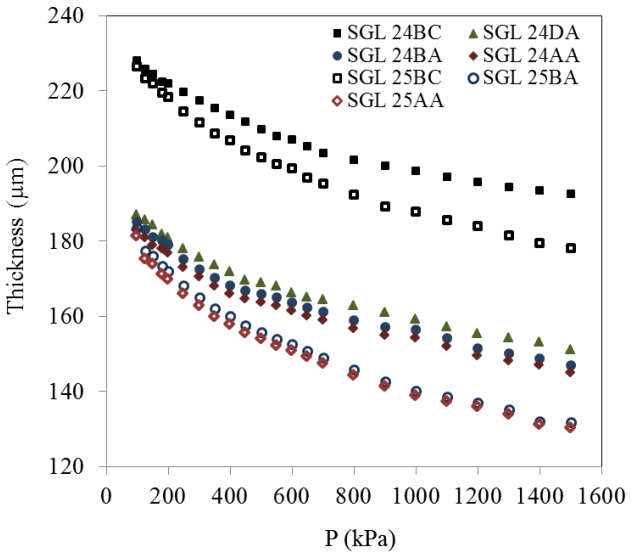

Fig. 11: Variations in thickness of GDLs with compression

5- CONCLUSION

Thermal conductivity of 14 SGL GDLs and its thermal contact resistance with iron clamping surfaces was modeled and measured at the temperature of around 60°C at a compression range of 2-14 bar. The results showed that:

- both PTFE and MPL reduce thermal conductivity (even though porosity decreases)
- both PTFE and MPL increase the contact resistance of GDLs with iron surfaces.
- MPL increases the contact resistance dramatically compared to untreated GDLs or GDLs with low PTFE content.

Having measured the thermal conductivity of GDLs coated with MPL, the thermal contact resistance between the MPL and the GDL substrate was measured. The results showed that the contact resistance of MPL with substrate is not negligible, and this resistance along with the MPL resistance, contributing almost equally, comprise altogether half of the GDL total resistance.

In addition to the experimental measurements, a new analytical robust model was developed that can accurately

predict the thermal conductivity of GDLs treated with PTFE. The model captures the trend of the experimental data and takes all the salient geometrical parameters, compression, and PTFE distribution inside the GDL.

ACKNOWLEDGMENTS

The Natural Sciences and Engineering Research Council of Canada (NSERC) for financial support of this work is acknowledged.

REFERENCES

[1] EG&G technical services, Fuel Cell Handbook. Parsons, Inc., Morgantown, West Virginiak, 2000.

[2] M.M., Mench, Fuel Cell Engines, John Wiley & Sons, 2008.

[3] A., Radhakrishnan, Thermal Conductivity Measurement of Gas Diffusion Layer Used in PEMFC, M.S. thesis, Rochester University, USA, 2009.

[4] D.L., Wood, R.L., Borup, 2009. Durability Aspects of Gas-Diffusion and Microporous Layers, in: Felix N. Büchi, Minoru Inaba, Thomas J. Schmidt (editors.), Polymer Electrolyte Fuel Cell Durability, Springer, New York, pp. 159-195. DOI: 10.1007/978-0-387-85536-3.

[5] N., Djilali, Computational modelling of polymer electrolyte membrane (PEM) fuel cells,Challenges and opportunities, Energy 32 (2007) 269–280.

[6] K.J., Lange, P.C., Sui, N., Djilali, Determination of effective transport properties in a PEMFC catalyst layer using different reconstruction algorithms, Journal of Power Sources 208 (2012) 354-365.

[7] B., Markicevic, N., Djilali, Analysis of liquid water transport in fuel cell gas diffusion media using two-mobile phase pore network simulations, J. Power Sources 196(5) (2011) 2725-2734.

[8] N.A., David, P.M., Wild, J., Hu, N., Djilali, In-Fibre Bragg Grating Sensors for Distributed Temperature Measurement in a PEM Fuel Cell, J. Power Sources 192 (2009) 376-380.

[9] N., Djilali, D., Lu, Influence of heat transfer on gas and water transport in fuel cells, International Journal of Thermal Sciences 41 (2002) 29–40.

[10] A., Tamayol, F., McGregor, M., Bahrami, Single phase through-plane permeability of carbon paper gas diffusion layers, J. Power Sources 204 (2012) 94-99.

[11] A., Tamayol, M., Bahrami, Water permeation through gas diffusion layers of proton exchange membrane fuel cells, J. Power Sources 196 (2011) 6356-6361.

[12] N., Zamel, E., Litovsky, X., Li, J., Kleiman, Measurement of the through-plane thermal conductivity of carbon paper diffusion media for the temperature range from -50 to +120 ^{o}C, International Journal of Hydrogen Energy 36 (2011) 12618-12625.

[13] N., Zamel, E., Litovsky, S., Shakhshir, X., Li, J., Kleima, Measurement of in-plane thermal conductivity of carbon paper diffusion media in the temperature range of -20 ^{o}C to +120 ^{o}C, Applied Energy 88 (2011) 3042–3050.

[14] G., Karimi, X., Li, P., Teertstra, Measurement of through-plane effective thermal conductivity and contact resistance in PEM fuel cell diffusion media, Electrochimica Acta 55 (2010) 1619–1625.

[15] M., Khandelwal, M.M., Mench, J. Power Sources 161 (2006) 1106–1115.

[16] O., Burheim, J.G., Pharoah, H., Lampert, J. Fuel. Cell Sci. Tech. (2011) doi: 10.1115/1.4002403.

[17] O., Burheim, P.J.S., Vie, J.G., Pharoah, S., Kjelstrup, J. Power Sources 195 (2010) 249-256.

[18] J., Yablecki, A., Bazylak, Determining the effective thermal conductivity of compressed PEMFC GDLs through thermal resistance modelling, Journal of Power Sources 217 (2012) 470-478.

[19] Z., Fishman, A., Bazylak, J., Electrochem. Soc. 158 (2011) B841-B845.

[20] H., Sadeghifar, M., Bahrami, N., Djilali, A statistically-based thermal conductivity model for fuel cell gas diffusion layers, Journal of Power Sources 233 (2013) 369-379.

[21] E., Sadeghi, M., Bahrami, N., Djilali, Analytic determination of the effective thermal conductivity of PEM fuel cell gas diffusion layers, Journal of Power Sources 179 (2008) 200–208.

[22] A., Pfrang, D., Veyret, G., Tsotridis, Computation of Thermal Conductivity of Gas Diffusion Layers of PEM Fuel Cells, Convection and Conduction Heat Transfer, Amimul Ahsan (Editor), ISBN: 978-953-307-582-2, InTech, (2011).

[23] M., Bahrami, M.M., Yovanovich, J.R., Culham, A compact model for contact of rough spheres, ASME Journal of Tribology, 127 (2005) 884–889. [24] SGL Group – The Carbon company. SIGRACET diffusion media, manufacture data sheet. Web: http://www.sglgroup.com/cms/international/home.

[25] G., Unsworth, N., Zamel, X., Li, Through-plane thermal conductivity of the microporous layer in a polymer electrolyte membrane fuel cell, International Journal of Hydrogen Energy 37 (2012) 5161-5169.

[26] J.D., Sole, investigation of novel gas diffusion media for application in PEM fuel cell ribbon assemblies. M.S. thesis, Virginia Polytechnic Institute and State University, USA, 2005.

[27] M.M., Mench, E., Caglan Kumbur, T.N., Veziro glu (editors), Polymer Electrolyte Fuel Cell Degradation, Academic press (Elsevier), MA, USA, 2012.

[28] N., Zamel, J., Becker, A. Wiegmann, Estimating the thermal conductivity and diffusion coefficient of the microporous layer of polymer electrolyte membrane fuel cells, Journal of Power Sources 207 (2012) 70– 80.

[29] P., Teertstra, G., Karimi, X., Li, Electrochimica Acta 56 (2011) 1670–1675.

[30] S.F., Burlatsky, W., Atrazhev, M., Gummalla, D.A., Condit, F., Liu, Journal of Power Sources 190 (2009) 485–492.

[31] K., Kang, H., Ju, Journal of Power Sources 194 (2009) 763–773.

[32] Standard Test Method for Thermal Transmission Properties of Thermally Conductive Electrical Insulation

Materials, ASTM Standard D-5470–06, ASTM International, Conshohocken, PA, 2007.

[33] E., Sadeghi, N., Djilali, M., Bahrami, Effective thermal conductivity and thermal contact resistance of gas diffusion layers in PEM fuel cells. Part 1: Effects of compressive load, Journal of Power Sources 196 (2011) 246-254.

[34] E., Sadeghi, N., Djilali, M., Bahrami, Effective thermal conductivity and thermal contact resistance of gas diffusion layers in PEM fuel cells. Part 2: Hysteresis Effect under Cyclic Compressive Load, Journal of Power Sources 195 (2010) 8104-8109.

[35] E., Sadeghi, N., Djilali, M., Bahrami, A novel approach to determine the in-plane thermal conductivity of gas diffusion layers in proton exchange membrane fuel cells, Journal of Power Sources 196 (2011) 3565-3571.

[36] M., Bahrami, J.R., Culham, M.M., Yovanovich, G.E., Schneider, A scale analysis approach to thermal contact resistance, ASME J. of Heat Transfer 126 (2004) 896-905.

[37] M., Bahrami, J.R., Culham, M.M., Yovanovich, G.E., Schneider, Review of thermal joint resistance models for non-conforming rough surfaces, ASME Journal of Applied Mechanics Review 59 (2006) 1–12.

[38] M., Bahrami, M.M., Yovanovich, J.R., Culham, A compact model for contact of rough spheres, ASME Journal of Tribology 127 (2005) 884–889.

[39] M., Bahrami, M.M., Yovanovich, J.R., Culham, Thermal joint resistance of non-conforming rough surfaces with gas-filled gaps, Journal of Thermophysics and Heat Transfer 18 (2004) 326–332.

[40] M., Bahrami, J.R., Culham, M.M., Yovanovich, Thermal contact resistance: a scale analysis approach, ASME Journal of Heat Transfer 126 (6) (2004) 896–905.

[41] M., Bahrami, M.M., Yovanovich, J.R., Culham, Thermal contact resistance at low contact pressure: effect of elastic deformation, International Journal of Heat and Mass Transfer 48 (16) (2005) 3284-3293

[42] H., Sadeghifar, M., Bahrami, N., Djilali, Thermal conductivity of Sigracet gas diffusion layers and MPL: Part I. Effect of compression, PTFE, MPL, cyclic load and hysteresis behaviour, ASME 11th Fuel Cell Science, Engineering and Technology Conference, July 14-19, 2013, Minneapolis, MN, USA, Paper No. ES-FuelCell2013-18070 (accepted abstract).

[43] H., Sadeghifar, M., Bahrami, N., Djilali, Thermal conductivity of graphite bipolar plate and its thermal contact resistance with gas diffusion layers: Effect of compression, PTFE, MPL, and cyclic load, ASME 11th Fuel Cell Science, Engineering and Technology Conference, July 14-19, 2013, Minneapolis, MN, USA, Paper No. ES-FuelCell2013-18072 (accepted abstract).

[44] I., Nitta, O., Himanen, M., Mikkola, Thermal Conductivity and Contact Resistance of Compressed Gas Diffusion Layer of PEMFuel Cell